

Supplementary Information

Low-Cost, Scalable Aerogel Evaporator via Machine Learning-Assisted Steel Needle Templating for Solar Desalination

Xinhao Yan^{a,#}, Zhuo Liu^{a,b,#}, Ting Shu^a, Yuliang Zhang^{a,*}, Zhiyan Li^a, Rong Bao^a, Xueting Chang^a, Yanhua Lei^a, Xiaobo Chen^{c,*}

^a College of Ocean Science and Engineering, Shanghai Maritime University, Shanghai, 201306, P. R. China.

^b Logistics Engineering College, Shanghai Maritime University, Shanghai, 201306, P. R. China.

^c Division of Energy, Matter & Systems, School of Science and Engineering, University of Missouri – Kansas City, Kansas City, MO 64110, USA.

* Corresponding authors:

Yuliang Zhang. Email: ylzhang@shmtu.edu.cn;

Xiaobo Chen. Email: chenxiaobo@umkc.edu.

The two authors contributed equally to this work.

Note S1 Analysis of water contact angle on the bottom surface of the D1.4N8-GSA evaporator.

It should be noted that during sample preparation, localized protrusions inevitably form on the solution surface due to ice crystallization during the freezing process. These protrusions are removed by trimming after freeze-drying, which may introduce a certain degree of surface unevenness. To minimize the influence of macroscopic surface roughness on the wettability measurements, water droplet tests were therefore conducted on the bottom surface of the sample, which was in direct contact with the mold, free from trimming, and relatively flat and smooth. The results show that water droplets on the bottom surface are also rapidly absorbed within 28 ms, consistent with the behavior observed on the upper surface.

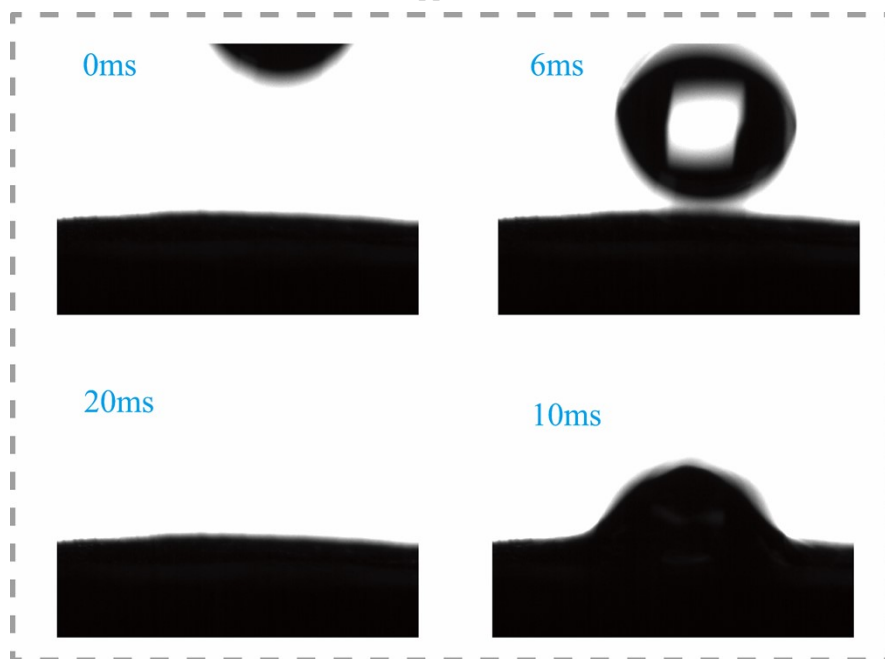


Fig. S1. Water contact angle image on the bottom surface of the D1.4N8-GSA evaporator.

Note S2. Heat loss analysis of the D1.4N8-GSA evaporator

Radiative heat loss

Radiative heat loss can be calculated by Stefan-Boltzmann law.

$$P_{rad} = \varepsilon\sigma(T_1^4 - T_2^4) \#(S1)$$

Where ε is the surface emissivity supposed as the maximum emissivity of 1, σ is the Stefan-Boltzmann constant (assumed to be $5.67 \times 10^{-8} \text{ W (m}^2 \cdot \text{K}^4)^{-1}$), T_1 (318.25 K) is the top surface temperature of D1.4N8-GSA evaporator at steady state under 1 sun illumination, and T_2 (314.45 K) is the ambient temperature upward the D1.4N8-GSA evaporator under 1 sun illumination. As a result, the radiation heat is estimated to be 27.28 W/m^2 , the radiation loss is about 2.7 %.

Convective heat loss

Convective heat loss can be calculated by Newton's law of cooling.

$$P_{conv} = h(T_1 - T_2) \#(S2)$$

where P_{conv} denotes convection heat flux, h is the convection heat transfer coefficient ($5 \text{ W (m}^2 \cdot \text{K)}^{-1}$). As a result, the convection heat is estimated to be 19 W/m^2 , and the convective heat loss is about 1.9 %.

Conductive heat loss

The conductive heat loss is calculated from the temperature gradient and the Fourier law:

$$P_{cond} = (A_1/A)Q_{water} \#(S3)$$

$$Q_{water} = k(\Delta T/\Delta L) \#(S4)$$

Where A_1 represents the direct contact area between the water and the evaporator, A denotes the effective cross-sectional area for heat transfer calculated based on the projected area of the evaporator, Q_{water} refers to the heat loss transferred to the bulk water, and ΔL is the effective heat conduction path length (here taken as 2/3 of the aerogel height). Due to water occupation within the structure, the thermal conductivity k is closed to water ($0.599 \text{ W/m} \cdot \text{K}^{-1}$), the $\Delta T/\Delta L$ is approximate 190 K/m and A_1/A was estimated to be 0.3125. Thus, the conductive loss is about 35.56 W/m^2 and the conductive heat loss rate is about 3.5 %.

Convective and radiative heat losses from the side surface of the evaporator

The heat loss from the side surface of the D1.4N8-GSA evaporator exposed to air mainly originates from convective and radiative heat losses. The conductive heat transfer from the side surface in contact with water has been incorporated into the conductive heat loss to the bulk water to avoid double counting.

$$P_{side} = P_{side,rad} + P_{side,conv} \#(S5)$$

where the radiative heat loss from the side surface ($P_{side,rad}$) and the convective heat loss from the side surface ($P_{side,conv}$) were calculated according to Equations S1 and S2, respectively. T_1 (307.95 K) is the steady state side surface temperature of the D1.4N8-GSA evaporator under 1 sun irradiation (Fig. S2), and T_2 (305.34 K) is the ambient temperature under the same conditions. Accordingly, $P_{side,rad}$ and $P_{side,conv}$ are estimated to be approximately 1.7 % and 1.3 %, respectively, yielding a total side surface heat loss (P_{side}) of about 3 %.

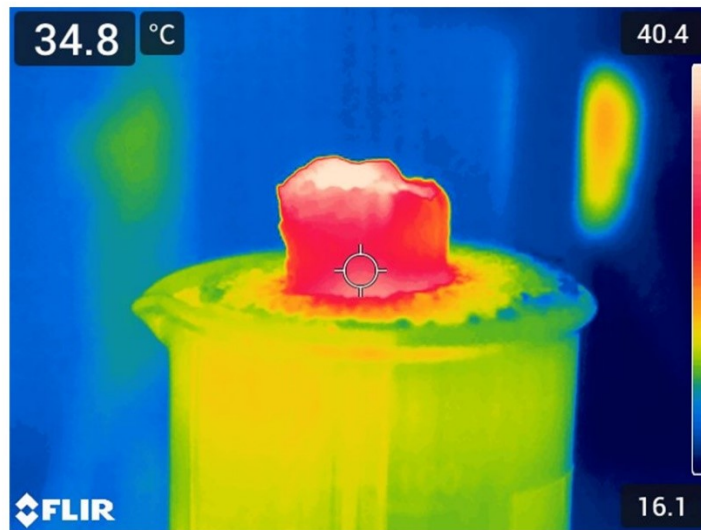


Fig. S2. The D1.4N8-GSA evaporator side temperature under 1 sun irradiation during steady state evaporation

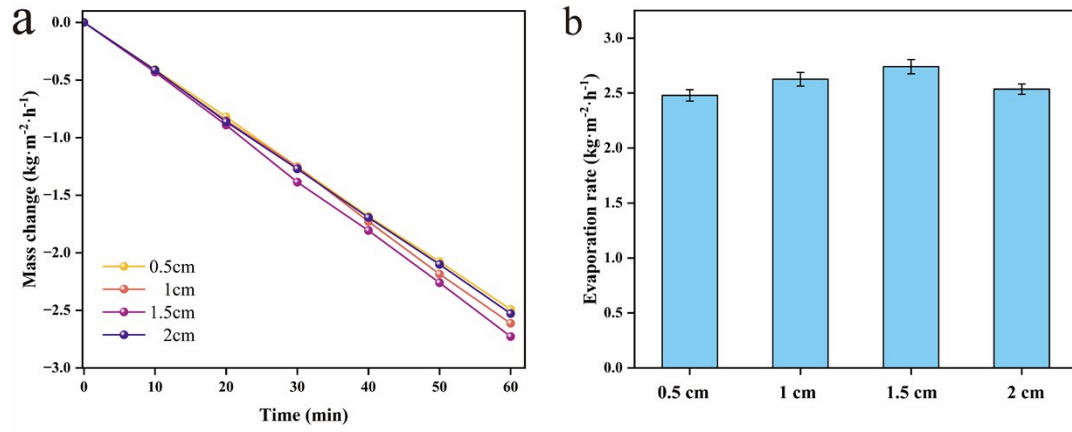


Fig. S3. (a) Mass change of evaporation rates of D1.4N8-GSA evaporator with different exposure heights. (b) Evaporation rates of D1.4N8-GSA evaporator with different exposure heights.



Fig. S4. Actual size photo of LD1.4N14-GSA Evaporator

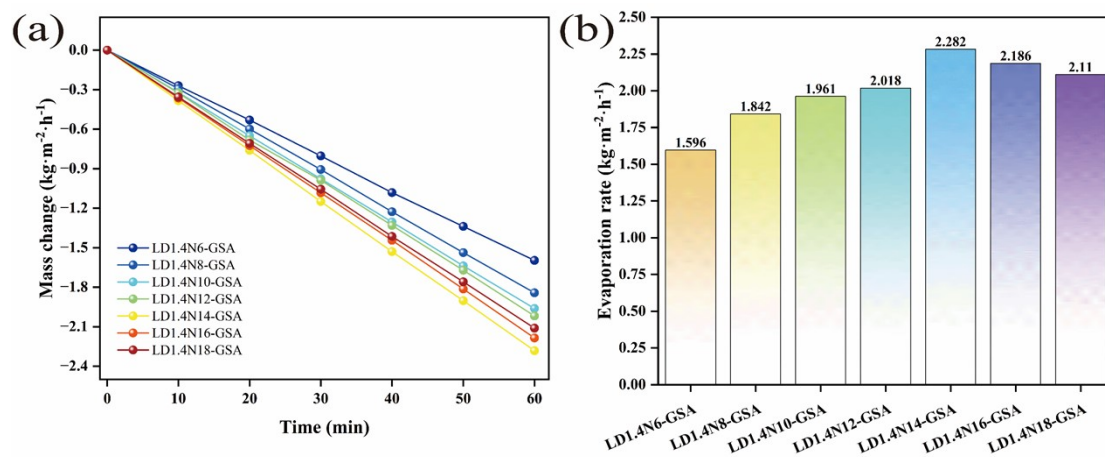


Fig. S5. (a) Mass change of LD1.4N-GSA evaporators within 1 hour under 1 kW·m⁻² irradiation with varying numbers of steel needles. (b) Comparison of LD1.4N-GSA evaporation rates within 1 hour under 1 kW·m⁻² irradiation with varying numbers of steel needles.

Note S3. Cost analysis of UF-GSA and D1.4N8-GSA evaporator**Table S1.** The price of raw materials (A.R.) for preparing UF-GSA and D1.4N8-GSA evaporator from Sinopharm Chemical Reagents Co., Ltd in China.

Raw materials	Quality	Price (\$)
Liquid nitrogen	1 L	1.42
Stainless steel needle (1.4 mm)	2 m	1.71
Sodium alginate	500 g	22.71
Graphene oxide	1 g	21.28
Anhydrous calcium chloride	500 g	2.67

Table S2. The cost of producing a UF-GSA evaporator with a diameter of 2.5 cm and a height of 3 cm

Materials	Quality	Price (\$)
Liquid nitrogen	800 ml	1.136
Sodium alginate	0.75 g	0.034
Graphene oxide	0.04 g	0.85
Anhydrous calcium chloride	3.5 g	0.019
Total: \$2.036		

Table S3. The cost of producing a D1.4N8-GSA evaporator with a diameter of 2.5 cm and a height of 3 cm

Materials	Quality	Price (\$)
Stainless steel needle (1.4 mm)	56 cm	0.48
Sodium alginate	0.75 g	0.034
Graphene oxide	0.04 g	0.85
Anhydrous calcium chloride	3.5 g	0.019
Total: \$1.383		

According to Table S1, S2 and S3, the direct material costs for fabricating a single UF-GSA and D1.4N8-GSA evaporator are approximately \$2.036 and \$1.383, respectively, indicating that the difference in per-unit raw material cost between the two approaches is not significant. However, in practical applications and large-scale fabrication scenarios, the overall economic viability of an evaporator is not determined solely by one-time material expenses; more decisive factors include the consumption of expendable materials, energy input, storage requirements, and the reusability of key components. Specifically, the conventional unidirectional freezing method relies heavily on liquid nitrogen as a cryogenic cooling medium. Liquid nitrogen is a continuously consumed material with a relatively high intrinsic cost and requires specialized cryogenic storage containers as well as a stable supply system. Under long-term operation or large-scale production conditions, these requirements inevitably introduce substantial hidden costs and additional operational burdens, thereby significantly increasing the overall fabrication cost. In contrast, in the steel needle templating strategy employed in this work, the stainless-steel needles serve solely as physical shaping templates and exhibit excellent structural stability and reusability, allowing them to be

repeatedly used over multiple fabrication cycles without frequent replacement. In addition, stainless-steel needles can be stored for extended periods under ambient conditions, resulting in negligible storage costs. Therefore, from the perspectives of long-term operation and large-scale manufacturing, the steel needle templating method demonstrates a clear advantage in overall cost control.